Chemosphere 341 (2023) 140046

Contents lists available at ScienceDirect

Chemosphere

journal homepage: www.elsevier.com/locate/chemosphere

Identification of organic micro-pollutants in surface water using MS-based infrared ion spectroscopy

Kas J. Houthuijs [a], Marijke Horn [a], Dennis Vughs [b], Jonathan Martens [a], Andrea M. Brunner [b,c], Jos Oomens [a,d], Giel Berden [a,*]

[a] Radboud University, Institute for Molecules and Materials, FELIX Laboratory, Toernooiveld 7, 6525 ED, Nijmegen, the Netherlands
[b] KWR Water Research Institute, Chemical Water Quality and Health, P.O. Box 1072, 3430 BB, Nieuwegein, the Netherlands
[c] TNO, Environmental Modelling, Sensing and Analysis (EMSA), Princetonlaan 8, 3584 CB, Utrecht, the Netherlands
[d] van't Hoff Institute for Molecular Sciences, University of Amsterdam, Science Park 904, 1098 XH, Amsterdam, the Netherlands

HIGHLIGHTS

- IR ion spectroscopy provides a structural fingerprint for *m/z*-features of pollutants.
- A workflow for pollutant identification with IRIS is presented.
- Screening of candidate pollutants is based on computed IR fingerprints.
- Candidate structures are derived from IR and MS/MS data and domain knowledge.

GRAPHICAL ABSTRACT

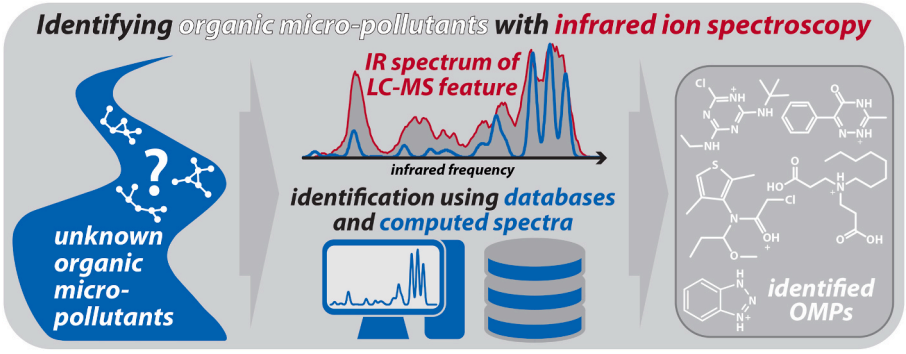

ARTICLE INFO

Handling Editor: J. de Boer

Keywords:
Organic micro-pollutants
Surface water
Molecular identification
Infrared ion spectroscopy
Non-target screening
Liquid chromatography-mass spectrometry

ABSTRACT

Comprehensive monitoring of organic micro-pollutants (OMPs) in drinking water sources relies on non-target screening (NTS) using liquid-chromatography and high-resolution mass spectrometry (LC-HRMS). Identification of OMPs is typically based on accurate mass and tandem mass spectrometry (MS/MS) data by matching against entries in compound databases and MS/MS spectral libraries. MS/MS spectra are, however, not always diagnostic for the full molecular structure and, moreover, emerging OMPs or OMP transformation products may not be present in libraries. Here we demonstrate how infrared ion spectroscopy (IRIS), an emerging MS-based method for structural elucidation, can aid in the identification of OMPs. IRIS measures the IR spectrum of an *m/z*-isolated ion in a mass spectrometer, providing an orthogonal diagnostic for molecular identification. Here, we demonstrate the workflow for identification of OMPs in river water and show how quantum-chemically predicted IR spectra can be used to screen potential candidates and suggest structural assignments. A crucial step herein is to define a set of candidate structures, presumably including the actual OMP, for which we present several strategies based on domain knowledge, the IR spectrum and MS/MS spectrum.

* Corresponding author.
E-mail address: g.berden@science.ru.nl (G. Berden).

https://doi.org/10.1016/j.chemosphere.2023.140046
Received 28 June 2023; Received in revised form 29 August 2023; Accepted 31 August 2023
Available online 1 September 2023

1. Introduction

The safety of drinking water sources is of paramount importance for public health and ecosystems (Bernhardt et al., 2017; Brack et al., 2022; Houthuijs et al., 2022; Villanueva et al., 2014). An important aspect concerns contamination caused by the ever-increasing production and use of chemicals, which find their way into the environment and eventually into water sources (Thompson et al., 2007). Organic micro-pollutants (OMPs) are anthropogenic chemicals such as agrochemicals, pharmaceuticals or chemicals related to industrial activity that occur at or below the microgram per litre level (Verliefde et al., 2007). Targeted approaches are employed to monitor the concentration of known OMPs, but due to their vast number and diversity, targeted detection of all OMPs is unfeasible. Moreover, OMPs can (bio)degrade to potentially more toxic transformation products (Schwarzenbach et al., 2006), which often remain undetected with a targeted approach. More comprehensive monitoring of OMPs can be achieved using non-target screening (NTS), which relies on a "detect-all" approach (Brunner et al., 2020; Campos-Mañas et al., 2019; Hollender et al., 2017; Hug et al., 2014; Ruff et al., 2015; Zheng et al., 2023). NTS is typically performed with liquid chromatography coupled to high-resolution mass spectrometry (LC-HRMS), which can cover both a wide range of chemical classes and a high dynamic range of concentrations, often reaching down to levels of ng/L (Brunner et al., 2020).

Obtaining the full molecular structure of an OMP with high confidence (Schymanski et al., 2014) is essential for risk assessment of its health and environmental impact. To this end LC-HRMS is routinely extended with tandem MS approaches, such as collision induced dissociation (CID) or ultraviolet photodissociation (UVPD) (Köppe et al., 2023; Panse et al., 2020; Zheng et al., 2023). MS/MS fragmentation spectra are then typically compared to (in-house) libraries for their identification. These MS/MS libraries, however, are incomplete, and frequently miss emerging OMPs and previously unknown transformation products. To alleviate this deficiency, *in silico* fragmentation tools are used to predict MS/MS spectra (Ruttkies et al., 2016; Wang et al., 2021), but these tools are often not sufficiently accurate to unequivocally identify unknowns (CASMI, 2022; Kiefer et al., 2021). Moreover, MS/MS spectra may be insensitive to small structural differences, such as positional isomerism (Crotti et al., 2021; Vink et al., 2022). Alternatively, nuclear magnetic resonance (NMR) spectroscopy can be used to identify OMPs, but limitations in selectivity and sensitivity compared to MS restrict its applicability to samples where micrograms of a relatively pure compound are available. Identification via NMR spectroscopy therefore requires extensive pre-concentration and purification steps, making its use for complex and low-abundance samples laborious.

Infrared (IR) spectroscopy presents an alternative tool towards molecular structure identification, providing information on the functional groups present in the unknown. To this end, gas chromatography (GC) coupled with FTIR absorption spectroscopy has been used together with GC-MS to identify environmental contaminants (Richardson et al., 1996; Thruston et al., 1991). However, direct absorption spectroscopy techniques cannot be directly coupled to MS such that they take advantage of the mass-spectral separation, thereby limiting their applicability.

Recently, infrared ion spectroscopy (IRIS) has seen application as an analytical technique to structurally identify (LC separated) m/z-features by recording their gas-phase IR spectra (Martens et al., 2020). Using a tuneable IR laser source, it is possible to perform wavelength-selective photodissociation of mass-selected ions. A series of IR-induced dissociation MS/MS spectra are recorded at different wavelengths in order to reconstruct the IR spectrum of the isolated ion. Since IRIS is directly integrated with MS, it inherits typical MS sensitivity (down to nM range), m/z-selectivity and the ability to couple to LC, making it an ideal method to identify low-abundant compounds in complex mixtures (Martens et al. 2017, 2020). IRIS has been applied for the identification of unknowns in domains such as biomarker discovery (Engelke et al., 2021), drug metabolism (van Outersterp et al., 2022), designer drugs (Kranenburg et al., 2020), agrochemicals and their transformation products (Vink et al., 2022) and organic molecules in secondary organic aerosols (Walhout et al., 2019). In fact, molecules from many of these domains are also found as OMPs in surface water, but their identification from surface water samples is more challenging since it is unknown *a priori* from which domain they originate.

An important feature of IR-based identification is that vibrational spectra can be reliably predicted using routine quantum-chemical methods, in sharp contrast to CID MS/MS fragmentation spectra. This often circumvents the strict requirement for chemical reference standards, as unknowns can be (tentatively) assigned based on their computed IR spectra. Multiple candidate compounds can thus be screened efficiently based on matching their predicted spectra with the spectrum of the unknown. The recent development of an *in silico* IR spectral library of molecular ions based on the human metabolome database (HMDB) further exploits the use of predicted vibrational spectra to aid in the identification of unknowns (Houthuijs et al., 2023). Not only can searching the library with an unknown's IR spectrum lead to direct identification, it can also yield molecular structures highly similar to the unknown, opening a path towards *de novo* structural elucidation.

Here, in a series of proof-of-principle experiments, we demonstrate the workflow for orthogonal identification of OMPs from surface water using IRIS. We will present data to show analytical reproducibility, identification strategies that rely on several libraries and how IRIS can be used in combination with MS/MS data to assign chemical structures.

2. Materials and methods

2.1. Sampling and sample preparation

The surface water sample was taken from the river Meuse, Roosteren, The Netherlands (June 11, 2018), in a stainless-steel container that was thoroughly washed and rinsed before sampling. The water sample was stored at 4 °C in the dark for a maximum of 1 week. A full description of the sample preparation is available in the supporting information (SI). In short, the surface water was guided across Oasis-HLB solid phase extraction (SPE) columns. The SPE cartridges were subsequently eluted using acetonitrile and reconstituted in ultrapure water (final concentration factor ~800x; final volume 1 mL) for LC-HRMS analysis and fraction collection.

2.2. UHPLC-HRMS/MS and fraction collection

Surface water samples were analysed in positive electrospray ionization mode using reverse phase LC-HRMS/MS and a Vanquish UHPLC system (Thermo Fisher Scientific, Bremen, Germany) and Tribrid Orbitrap Fusion mass spectrometer (Thermo Fisher Scientific, Bremen). An XBridge C18 XP column (2.1 mm × 150 mm I.D., 2.5 μm particle size, Waters, Etten-Leur, The Netherlands) was used combined with a SecurityGuard Ultra column (2.0 mm × 2.1 mm I.D., Phenomenex, Torrance, USA) and kept at 25 °C. The LC gradient was varied from 5% acetonitrile and 95% water with 0.05% formic acid (v/v/v) to 100% acetonitrile with 0.05% formic acid in 25 min and then retained for 4 min, all with a 250 μL/min flow rate. Mass spectra were acquired in the m/z 80–1300 range with a resolving power at m/z 200 of 120 000 full width at half maximum (FWHM). Data dependent acquisition of MS/MS spectra was performed with high-energy collisional dissociation (HCD) energy at 35% and a resolving power of 15 000 FWHM.

Data analysis for nontarget screening was performed using Compound Discoverer 3.0 (Thermo Fisher Scientific) for peak picking, componentization, and automatic MS/MS fragment searches in mzCloud and our in-house library. Based on their relatively high abundance, three known (OMPs 1–3) and two unknown compounds (OMPs 4–5) were selected for IRIS analysis (see Table 1).

Table 1
Overview of compounds analysed with infrared ion spectroscopy. The labels OMP1-OMP5 refer to compounds from the Meuse river sample. The labels REF1 and REF2 refer to reference compounds, which were not analysed with LC-HRMS/MS.

label	exp. *m/z*	adduct	Δm (ppm)	RT (min.)	name
OMP1	230.1163	$[C_9H_{16}ClN_5+H]^+$	−1.7	16.9	terbuthylazine
OMP2	120.0554	$[C_6H_5N_3+H]^+$	−1.9	7.9	benzotriazole
OMP3	276.0816	$[C_{12}H_{18}ClNO_2S+H]^+$	−1.3	17.3	dimethenamid
OMP4	188.0817	$[C_{10}H_9N_3O+H]^+$	−0.7	8.7	metamitron-desamino
OMP5	274.2008	$[C_{14}H_{27}NO_4+H]^+$	−1.6	10.8	N-(2-carboxyethyl)-N-octyl-β-alanine
REF1	–	$[C_{15}H_{23}O_3–H]^-$	–	–	gemfibrozil
REF2	–	$[C_9H_9O_3Cl–H]^-$	–	–	2-methyl-4-chlorophenoxyacetic acid

LC-IRIS analysis can be performed online (van Outersterp et al., 2023), but since a different LC-MS platform was used for non-target screening, a fractionation approach was employed for the IRIS analysis, which ensures that the same compounds were sampled. For fractionation, 100 μL of the ultrapure water diluted extract was injected, after which fractions of approximately 0.3 min around the target retention time were collected in an autosampler vial. Four fractions per time window were collected in a single vial to which another 150 μL of acetonitrile was added, resulting in an extract of about 400 μL for identification using IRIS.

2.3. Infrared ion spectroscopy

IR spectra of the OMPs (listed in Table 1) and reference standards were measured on an AmaZon Speed ETD quadrupole ion trap mass spectrometer (Bruker, Bremen, Germany) (Martens et al., 2016), which has been coupled to the beamline of the infrared free-electron laser FELIX (Oepts et al., 1995). The collected LC-fractions of OMPs and prepared reference standard solutions (1–10 μM) were measured using direct injection at a flowrate of 120–180 μL/h and ionized using electrospray ionization (sample consumption for recording a single IR spectrum is 14–30 μL). After *m/z*-isolation of the feature of interest, or their fragment ions produced by CID, the ions were irradiated with 1 macropulse of FELIX, which was operated at a 10 Hz repetition rate. Each 10 μs macropulse had an energy of 10–200 mJ and a bandwidth of approximately 0.5% of the centre frequency. The wavelength dependent absorption of IR photons increases the internal energy of the isolated ions until their dissociation threshold is reached and the precursor ions fragment. The wavelength-dependent fragmentation observed in the recorded mass spectra is converted into an IR spectrum by plotting the fragmentation yield, defined as $-\ln[I_{precursor} / \sum(I_{all})]$, as a function of IR frequency. The yield is linearly corrected for the wavelength dependent IR laser pulse energy (Berden et al., 2019). The IR wavelength is calibrated using a grating spectrometer.

2.4. Computational workflow

A computational workflow based on RDKit and Gaussian16 was employed for the computation of IR spectra (Frisch et al., 2016; Landrum, 2006; van Outersterp et al., 2019). The input for the workflow consists of the 2D-representation of each candidate structure in SMILES notation (Weininger, 1988). Iterating through all possible tautomers of the neutral molecule, ionized structures were devised by either protonating or deprotonating the available hetero-atoms. For each resulting ion, 500 random conformations were generated and subsequently minimized using the MMFF94 classical force field implemented in RDKit (Halgren, 1996; Tosco et al., 2014). After clustering of the final geometries, a maximum of 20 distinct geometries were selected (or fewer) as determined by a root-mean-square deviation threshold of 1.4 Å (Ebejer et al., 2012). The selected 3D-geometries were submitted to a geometry optimization and frequency calculation at the semi-empirical PM6 level using Gaussian16. Higher-energy structures were removed based on a 40 kJ mol^{-1} cut-off and identical geometries were filtered based on their computed IR frequencies and intensities. The remaining geometries were reoptimized at the B3LYP/6–31++G(d,p) level, followed by a harmonic frequency calculation (Stephens et al., 1994). After scaling (0.975) of the frequencies, the vibrational stick spectra are convoluted with a 45 cm^{-1} Gaussian broadening function. Finally, a single-point energy calculation is performed for each final geometry using second-order Møller-Plesset perturbation theory (MP2). This electronic energy was combined with entropic and enthalpic contributions from the B3LYP vibrational analysis to yield Gibbs free energies (T = 298 K). The computed spectrum of the lowest-energy geometry for each structure was used for the spectral comparison against experimental spectra, unless stated otherwise.

2.5. Scoring of spectral similarity

To quantify the match between two spectra, the cosine similarity score is employed. Experimental and computed spectra are represented as vectors of spectral intensities (**a** and **b**). The similarity *S* is defined as the Euclidean dot product of spectra **a** and **b** multiplied by 1000:

$$S = 1000 \bullet \frac{\boldsymbol{a} \bullet \boldsymbol{b}}{|\boldsymbol{a}||\boldsymbol{b}|} = 1000 \bullet \frac{\sum_{i=1}^{n} a_i b_i}{\sqrt{\sum_{i=1}^{n} (a_i)^2}\sqrt{\sum_{i=1}^{n} (b_i)^2}}$$

where a score closer to 1000 indicates greater similarity. To ensure a common x-axis, the intensities of the computed spectra are evaluated at the frequency points of the experimental spectrum. Before computing the similarity, the intensities of both spectra are transformed by taking their square root:

$$I_i^{transformed} = \sqrt{I_i}$$

This reduces the weight of the more intense peaks and increases that of peaks with lower intensity; it also makes *S* less sensitive to intensity deviations between experimental and computed spectra, and therefore more sensitive to frequency overlap (Houthuijs et al., 2023). The scoring algorithm is also used to quantify the similarity between two experimental spectra; in this case, a common x-axis is ensured by linearly interpolating the intensities of both spectra onto a common frequency scale with 1 cm^{-1} steps.

3. Results and discussion

3.1. IRIS of OMPs in river water: analytical reproducibility

First, we demonstrate the capability of IRIS to confirm the identity of OMPs. OMP1 and OMP2 (see Table 1) were assigned based on matching of their MS/MS spectra to an in-house library and external mzCloud library. Both OMPs were collected from surface water and fractionated using multiple LC runs as described above. Direct infusion of the collected fractions into the ion trap mass spectrometer enabled us to record their IRIS spectra. The IR spectrum of protonated OMP1, $[C_9H_{16}ClN_5+H]^+$, assigned to terbuthylazine (99.7% match using mzCloud), a herbicide and known water contaminant (Bottoni et al., 2013), is presented in Fig. 1a in grey. Overlaid on the spectrum is the IR spectrum of a terbuthylazine reference standard in black, as well as the

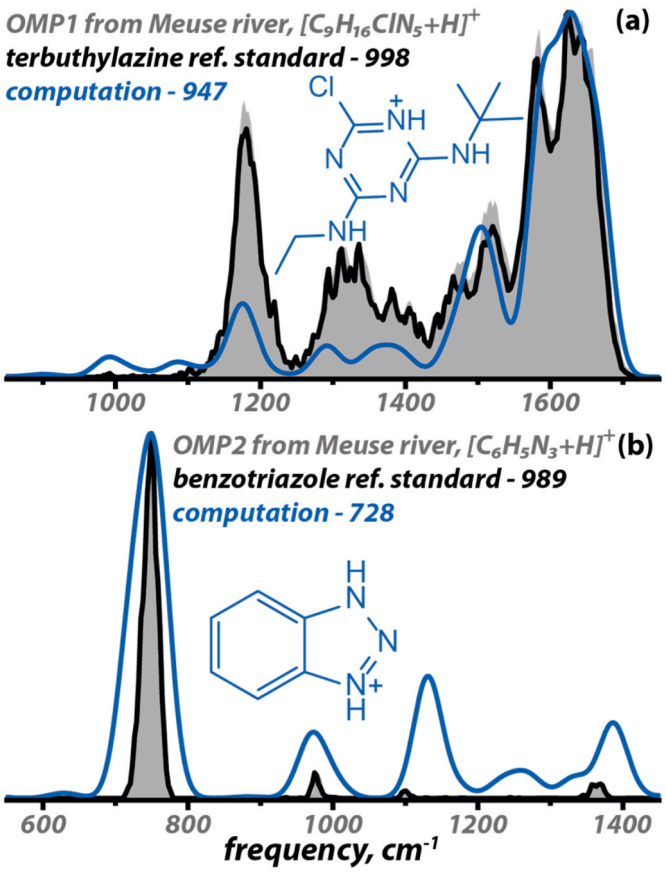

Fig. 1. Experimental IRIS spectra of protonated OMP1 (a) and OMP2 (b) in grey, compared with experimental IRIS spectra (black) as well as computed spectra (blue) of protonated terbuthylazine (a) and benzotriazole (b). Molecular structures as well as similarity scores are shown.

computed spectrum of protonated terbuthylazine in blue. The identification is confirmed by the almost exact match between the spectra of OMP1 and the reference standard, as indicated by a similarity score of 998. In addition, the similarity score of 947 between the computed spectrum of protonated terbuthylazine and the IR spectrum of OMP1 suggests that computed spectra can serve as an effective reference to achieve tentative assignments when physical standards are not available.

Similarly, the IR spectrum of protonated OMP2 ($[C_6H_5N_3+H]^+$), assigned to benzotriazole (99.4% using mzCloud), is presented in Fig. 1b in grey. Benzotriazole is commonly used as a corrosion inhibitor and was recently detected in water around the world (Alotaibi et al., 2015). Fig. 1b also presents the spectrum of the reference standard (black) and the computed spectrum (blue) of protonated benzotriazole. Again, an excellent match between the spectrum from the water sample and the reference spectrum is observed (similarity score of 989), thereby confirming the assignment of OMP2 to benzotriazole. In this case, however, the computed spectrum provides a poorer match, having a similarity score of only 728. Several peaks between 900 and 1400 cm^{-1} in the computed spectrum remain unobserved in the experimental spectrum, probably due to the high dissociation threshold of protonated benzotriazole. IR excitation at these weaker bands is inefficient and fails to increase the internal energy to above the fragmentation threshold, leaving these bands undetected in the IRIS spectrum. This demonstrates that care must be taken when using computational spectra as a reference and specifically that weak vibrational bands may be underrepresented in the experimental spectrum. The absolute similarity score is therefore not to be interpreted as a direct measure of structural identification, as true positives can have a wide range in scores (Houthuijs et al., 2023). Instead, the similarity score should be employed as a ranking of candidates, as is shown below.

3.2. Identification using in silico IR spectra

To identify OMPs, libraries of commonly used chemicals are often consulted. Such an approach can also be taken for their identification with IRIS, by considering common chemicals as candidate structures. This approach is demonstrated in Fig. 2, where the measured IR spectrum of deprotonated gemfibrozil, $[C_{15}H_{22}O_3–H]^-$, is presented in black. Gemfibrozil is a pharmaceutical for regulating lipid levels in blood and enters the environment via excretion in urine and feces (Fang et al., 2012). Here, we take this experimental IR spectrum as the spectrum of a

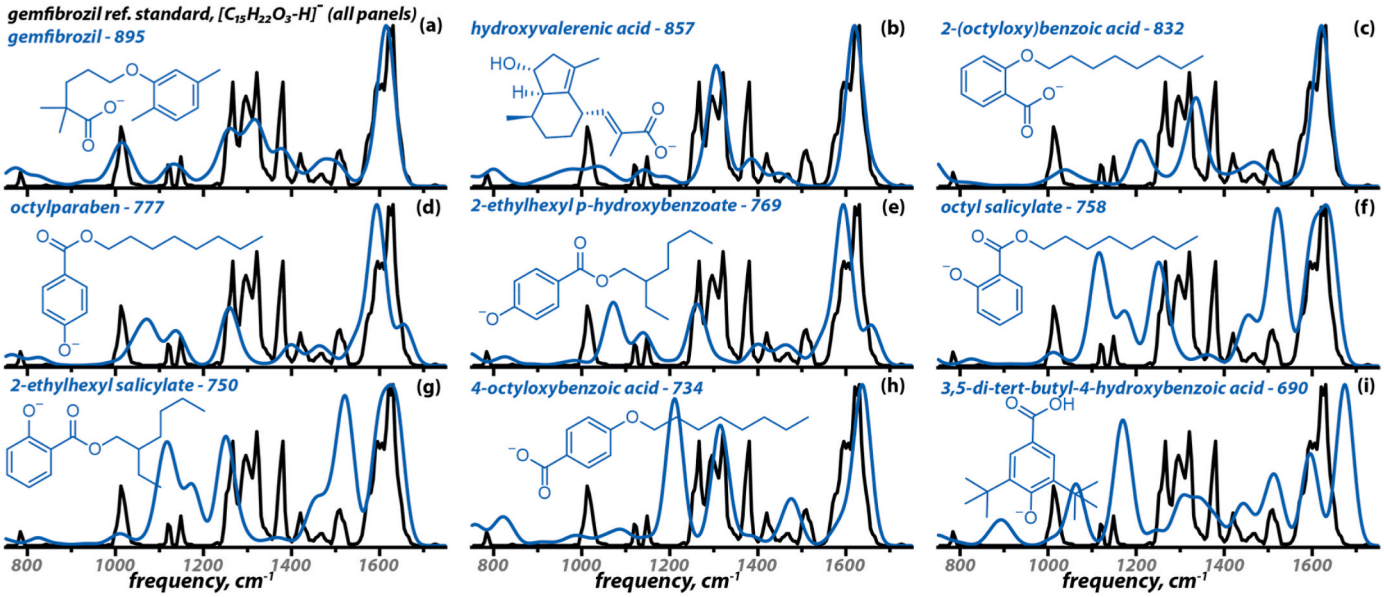

Fig. 2. Comparison of the experimental IR spectrum of deprotonated gemfibrozil (black) to the nine best matching computed spectra (blue) out of a set of ten compounds. The ten candidate structures derive from a CompTox chemicals dashboard search with the accurate mass (250.1569 Da ± 10 ppm) and selecting the 10 compounds with the highest number of associated data sources. Inscribed are the spectral matching scores and structures.

hypothetically unidentified OMP and investigate if we can retrieve its identity from the spectral and accurate mass information alone. The accurate mass of gemfibrozil (250.1569 Da ± 10 ppm) was used to search the CompTox Chemicals Dashboard (https://comptox.epa.gov/dashboard, accessed 2023/03/09) (McEachran et al., 2017), which yielded 244 compounds. From this list, the 10 chemicals with the highest number of associated data sources were selected (with gemfibrozil at #2, see Scheme S1 in the SI) and their vibrational spectra as deprotonated ions were computed. The rationale behind selecting on associated data sources is that commonly known or used molecules are more likely to be present in the environment, although this approach is counterproductive when looking for novel substances (Little et al., 2011). The 9 best matching spectra and associated structures are shown in Fig. 2, while all 10 can be seen in Figure S1 in the SI. Of the ten computed vibrational spectra, the spectrum of deprotonated gemfibrozil provides the best match (S = 895) with the experimental IR spectrum (Fig. 2a), thus successfully identifying gemfibrozil and demonstrating the structural specificity of IR spectroscopy for this set of isomeric structures. The computed spectrum of hydroxyvalerenic acid has a high similarity with the experimental spectrum (S = 857) as well, but shows clear spectral mismatch around 1510 cm^{-1}, 1250 cm^{-1} and 850-950 cm^{-1} (Fig. 2b). More generally, the broad peak around 1600 cm^{-1} matches well with the three best-scoring spectra; it corresponds to stretches of the carboxylate and alkene/aromatic functionalities. The position of the carboxylate within the molecule is further recognized to not be on the phenyl ring, as this gives rise to unique C–C vibrations within the ring at 1200 cm^{-1} (Fig. 2c and h), which are absent in the experimental spectrum.

For the proof-of-concept identification of gemfibrozil described above, we essentially generated a small reference library of *in silico* IR spectra of isomeric candidates. Alternatively, a more general molecular structure search can be conducted by employing a much larger *in silico* library, which was constructed in earlier work involving the Human Metabolome Database (HMDB) (Houthuijs et al., 2023). This library currently contains 75 941 computed IR spectra of ions derived from 4640 compounds and can be searched with or without *m/z* constraints. An unconstrained search enables the retrieval of general substructure motifs and thereby the (partial) structural elucidation of compounds absent in databases. This approach is demonstrated with the IR spectrum of deprotonated 2-methyl-4-chlorophenoxyacetic acid (MCPA, $[C_9H_9ClO_3–H]^-$), a widely used herbicide (Morton et al., 2020). Fig. 3a–c presents the IR spectrum of deprotonated MCPA in black and the three best matching computed spectra from the library. In this case, the search does not return MCPA itself, as it is not one of the 2707 deprotonated entries in the library. Instead, phenoxyacetic acid provides the best match with the experimental IR spectrum (S = 907, Fig. 3a). Experimental and computed spectra indeed show an excellent match, which reflects the significant structural similarity between phenoxyacetic acid (Fig. 3a) and MCPA (Fig. 3d). The Cl and CH_3 ring substitutions that differentiate both structures, have only limited influence on the IR spectrum in the probed wavenumber range.

What these results moreover demonstrate, is that even though the IR spectral library is based on the human metabolome database (HMBD), it can still be applied in fields outside of (human) metabolomics. That is, the HMDB is – just as any chemical database – a representation of chemical space. In addition, the HMDB also includes molecules associated with the human exposome, *i.e.* the molecules an individual is exposed to during their lifetime (Neveu et al., 2016; Wishart et al., 2018), and therefore also includes molecules found in surface water. Therefore the current version of the IR spectral library based on the HMDB could play a role in the identification of biotransformation products, until common anthropogenic chemicals are added from sources such as CompTox or the NORMAN suspect list (McEachran et al., 2017; Network et al., 2020).

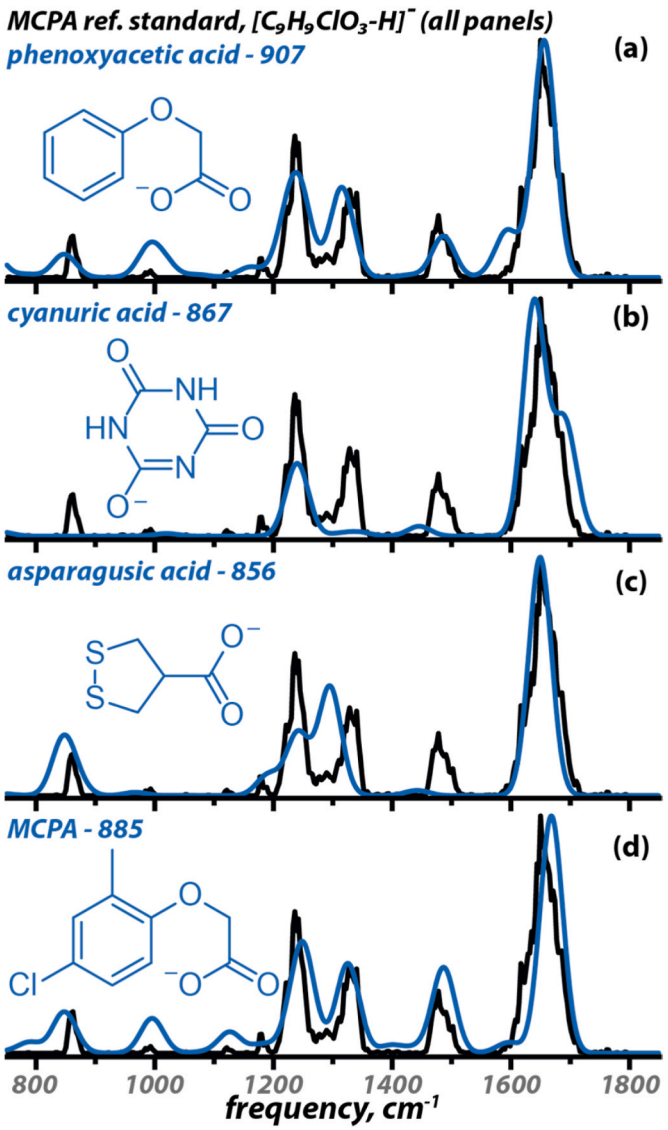

Fig. 3. (a–c) Top-3 matching results from a query of the *in silico* IR spectral library from (Houthuijs et al., 2023) using the experimental IRIS spectrum of deprotonated MCPA (black in all panels). Computed spectra (blue) are for the deprotonated ions of phenoxyacetic acid $[C_8H_8O_3–H]^-$ (a), cyanuric acid $[C_3H_3N_3O_3–H]^-$ (b) and asparagusic acid $[C_4H_6O_2S_2–H]^-$ (c). Panel (d) presents the computed spectrum of deprotonated MCPA ($[C_9H_9O_3Cl–H]^-$). Inlayed are the molecular structures as well as the similarity scores.

3.3. IR spectra of MS/MS fragment ions aid in identification

Although OMP3 could be identified based on LC-HRMS data alone, we use this case as an example where an extended workflow using detailed spectral information of the OMP and its MS/MS fragment ion lead to a successful identification. The IR spectrum of protonated OMP3, assigned to $[C_{12}H_{18}ClNO_2S + H]^+$ based on accurate mass, is presented in grey in Fig. 4a–c. Additionally, the high-resolution CID MS/MS spectrum of protonated OMP3 was recorded (Figure S2 in the SI), as well as the IR spectrum of the mass-isolated CID fragment ion, which is formed by loss of methanol giving an ion with elemental composition $[C_{11}H_{14}ClNOS + H]^+$ (grey spectrum in Fig. 4d and e). The precursor molecular formula was used to query the CompTox Chemicals Dashboard (accessed 2023/03/09), yielding 11 unique candidates after removing duplicates and enantiomers. Two of these structures contained a methoxy group that could explain the observed methanol loss after CID (see Scheme S2 in the SI). The computed spectra of these candidates, 2-

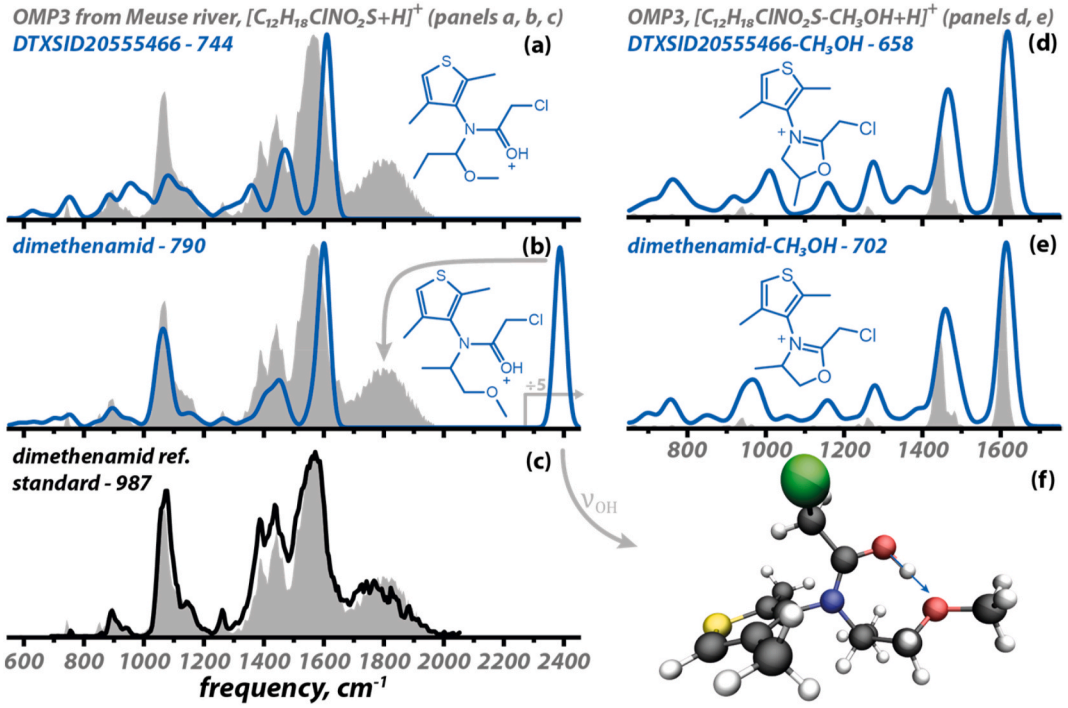

Fig. 4. Identification of OMP3 using the IR spectra (grey) of its protonated ion (a, b, c) and the methanol-loss fragment thereof (d, e). These spectra are compared against computed spectra (blue) of DTXSID20555466 (a) and dimethenamid (b), their respective methanol-loss fragments (d, e) and the IR spectrum of a reference standard (black) of dimethenamid (c). The OH stretch vibration calculated at 2400 cm^{-1} in (b) is visualized in (f), where the blue arrow indicates the main vibrational coordinate. Inlayed are the structures, as well as the similarity scores of the overlaid spectra.

chloro-*N*-(2,4-dimethylthiophen-3-yl)-*N*-(1-methoxypropyl)acetamide (CompTox label DTXSID20555466) and dimethenamid, are shown in blue in Fig. 4a and b.

The IR spectrum of the precursor ion features an unusually broad absorption band that extends from 1700 to almost 2000 cm^{-1}. This peak is not reproduced by the computed IR spectra of either of the candidates, although otherwise the experimental spectrum shows good overlap with the computed spectrum of dimethenamid (Fig. 4b). Closer inspection of its computed spectrum reveals a vibrational band with high integrated intensity (2330 km/mol) at 2400 cm^{-1}, corresponding to the stretching mode of the proton shared between the two O-atoms in the molecule (Fig. 4f). It is well known that the harmonic approximation applied here usually fails to describe the motion of shared protons in strongly hydrogen-bonded systems (Buckingham et al., 2008, Del Bene and Jordan, 1999). The vibrational band associated with this motion typically occurs at lower frequencies and is severely broadened (Gámez et al., 2021), and therefore possibly matches the observed broad feature centred at 1800 cm^{-1} (Fig. 4b).

To corroborate this assignment, the IR spectra of the most probable structures after methanol loss for DTXSID20555466 and dimethenamid were calculated and compared to the IR spectrum of the −32 Da neutral loss fragment of protonated OMP3 (Fig. 4d and e). All considered fragment structures and their computed IR spectra are presented in Figure S3 in the SI, along with proposed mechanisms for their formation in Schemes S3 and S4. An activation-induced rearrangement leads to methanol loss and yields the depicted cyclic structures, which is a common fragmentation mechanism in CID (Kempkes et al., 2016). This comparison provides further support for the assignment of OMP3 as dimethenamid, a herbicide found in surface water (Zimmerman et al., 2002), since the IR spectrum of the CID fragment ion matches best with the computed spectrum of its proposed methanol-loss structure.

Finally, we measured the IRIS spectrum for a dimethenamid reference standard, as presented in Fig. 4c in black. Comparison to the spectrum of protonated OMP3 shows great similarity between both spectra (S = 987), thereby definitively identifying OMP3 to be dimethenamid (level 1 structure identification (Schrimpe-Rutledge et al., 2016; Schymanski et al., 2014)).

3.4. Identification of unknown OMPs

In the previous examples an initial assignment was made based on in-house LC-MS reference standards. What follows is the identification of an OMP that could not be identified unambiguously based on LC-HRMS/MS. The IRIS spectrum of the protonated ion of OMP4, $[C_{10}H_9N_3O + H]^+$, was measured, as presented in grey in Fig. 5. To further exploit the information contained in the high-resolution MS/MS spectrum, we used the software Sirius (version 5.7.2) (Dührkop et al., 2019). Sirius uses machine learning to predict the molecular structure from an MS/MS spectrum. This prediction is in the form of a molecular fingerprint vector, but with probabilities instead of typical bits (Dührkop et al., 2015). By calculating the similarity of this prediction versus bit vectors of molecules in databases such as PubChem, a list of candidate molecules is returned that likely yield an MS/MS spectrum similar to the provided spectrum. This approach was applied to the MS/MS spectrum of OMP4 (Figure S4 in the SI) and the top-10 candidates are presented in Scheme S5 in the SI. The IR spectrum of each candidate was computed and the similarity to the IR spectrum of protonated OMP4 was determined. The top-5 matching computed spectra are presented in Fig. 5a–e in blue, where higher-energy structures were included up to 10 kJ mol^{-1} (Figure S5 in the SI). We demonstrated previously that considering computed spectra of higher-energy geometries can be essential for the correct assignment of the molecular structure (Houthuijs et al., 2023).

Although the ten structures returned by Sirius are all highly similar, their computed IR spectra are distinct (Fig. 5 and S5 in the SI). This demonstrates the orthogonality of tandem-MS and IR spectroscopy, underpinning the value of combining information from both sources.

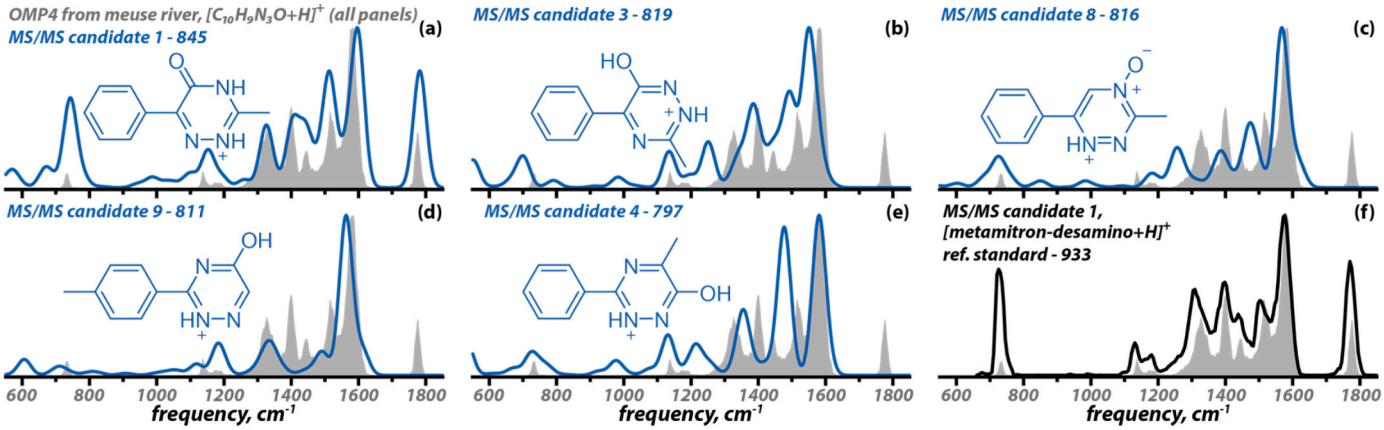

Fig. 5. Identification of OMP4 using the IR spectrum (grey) of its protonated ion. This spectrum is compared with the 5 best matching computed spectra (blue) of 10 MS/MS candidates (a–e) and the IR spectrum of a reference standard (black) of metamitron-desamino (f). Inlayed are the computed structures and the similarity scores of the overlaid spectra.

Looking at the top-5 matching candidates, only candidate #1 reproduces the carbonyl stretch in the experimental spectrum (at 1775 cm^{-1}) and has an overall good match with the remainder of the experimental spectrum (Fig. 5a). We recorded an IRIS spectrum for the reference standard of this candidate, metamitron-desamino, which showed a close match with protonated OMP4 (Fig. 5f), giving a similarity score of 933. Metamitron-desamino is a biotransformation product of metamitron, which is used as a herbicide for weed control in sugar beet crops (Wang et al., 2017).

For the identification of OMP4 it was crucial to also consider higher-energy structures, as protonated OMP4 adopts a tautomeric form that is computed to be 6.5 kJ mol^{-1} higher in energy than the lowest-energy tautomer (Figure S5 in the SI). The observation of higher-energy structures with IRIS is not uncommon, due to the limited accuracy of computed energies or to kinetic trapping of solution-phase tautomers (Steill and Oomens, 2009; Warnke et al., 2015). Relying solely on computed spectra of the lowest-energy geometries would have resulted in a tie between MS/MS candidates #1 and #3 (both S = 819), with both computational spectra showing clear mismatches with the experimental spectrum (panels a and b in Figure S5 in the SI). The spectrum of the higher-energy tautomer of pronated metamitron-desamino, however, has a higher similarity score (S = 845) and reproduces all experimental peaks.

Finally, to identify OMP5, we measured the IRIS spectrum of its protonated ion $[C_{14}H_{27}NO_4+H]^+$ and its fragment ion resulting from loss of neutral $C_2H_4O_2$ (Fig. 6a and b). The HRMS/MS spectrum (Figure S6) was again used to formulate candidates with Sirius. All top-10 candidates possess ester functional groups, as seen in Scheme S6 in the SI. However, querying the *in silico* spectral library with the IR spectrum indicates the presence of a carboxylic acid group substructure, based on the features at 1750 and 1150 cm^{-1}, which are characteristic –COOH vibrations (Figure S7 in the SI). This is further corroborated by the dominant neutral loss of $C_2H_4O_2$, which can be attributed to acetic acid. Querying the CompTox database (accessed 2023/06/09) using the neutral chemical formula ($C_{14}H_{27}NO_4$) yielded 25 structures, three of which possess a carboxylic acid functional group. N-(2-carboxyethyl)-N-octyl-β-alanine is used in washing and cleaning products and computed IR spectra for its protonated ion and its acetic acid loss fragment are shown in Fig. 6a and b. Both computed spectra show excellent agreement with the experimental IR spectra (S = 936 and S = 849) and we therefore identify OMP5 as N-(2-carboxyethyl)-N-octyl-β-alanine. Closer inspection of the Sirius results reveals N-(2-carboxyehtyl)-N-octyl-β-alanine to be ranked #198 (out of 2240). This demonstrates the power of the combined use of *in silico* MS/MS approaches and spectroscopic IRIS analysis in the annotation of unknown mass spectral features.

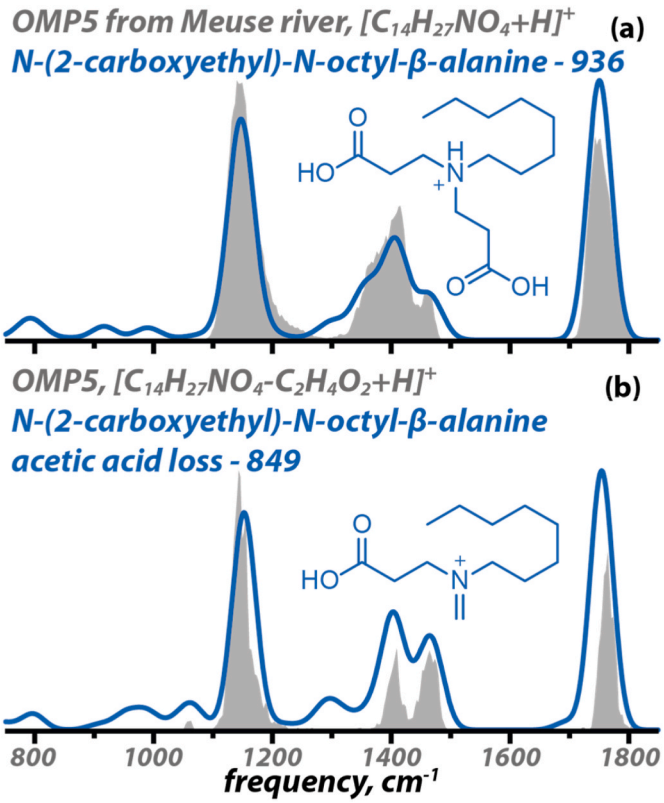

Fig. 6. Identification of OMP5 using the IR spectra (grey) of the protonated ion (a) and its CID fragment corresponding to loss of neutral acetic acid (b). The spectra are compared with computed spectra (blue) of protonated N-(2-carboxyehtyl)-N-octyl-β-alanine (a) and the proposed acetic acid loss structure (b). Inlayed are the computed structures and the spectral similarity scores of computed and experimental spectra.

4. Conclusions

We demonstrated that infrared ion spectroscopy (IRIS) can aid in the identification of organic micropollutants (OMPs) in surface water. As an extension of mass spectrometry, IRIS can be appended to analytical LC-MS workflows and can thus be employed for the identification of detected LC-MS features. The reproducibility of IRIS allows for the definitive structural assignment of detected OMPs by measuring reference standards (level 1 including an orthogonal method

(Schrimpe-Rutledge et al., 2016; Schymanski et al., 2014)), as was verified using a similarity scoring algorithm. In addition to analytical standards, quantum-chemically computed spectra can also serve as references to provide tentative but accurate suggested assignments in absence of analytical standards. Moreover, using a library of DFT-computed spectra, in the presented example based on the human metabolome database, OMP structures can be quickly identified; even for structures not included in the library, molecules closely related in structure can be identified.

We further demonstrated that a key step in the identification process is formulating a set of likely candidates. Computed IR spectra for these candidates then allow one to quickly exclude many candidates. Here, this resulted in two tentative assignments that were subsequently confirmed with chemical reference standards. In formulating such a candidate set, tandem mass spectrometry plays a crucial role. Additionally, IRIS can be applied to MS/MS fragments of LC-MS features, to further increase confidence in (tentative) assignments by comparing the IR spectrum against computed spectra of hypothesized CID fragment ion structures of candidates. We envision that the described set of approaches form a toolbox for IRIS-based structural elucidation. This toolbox can be employed in environmental sciences for the identification of detected OMPs at high confidence levels, as well as in other non-targeted, small-molecule LC-MS applications.

CRediT authorship contribution statement

Kas J. Houthuijs: Investigation, Visualization, Software, Writing – original draft. **Marijke Horn:** Investigation. **Dennis Vughs:** Investigation, Resources, Writing – review & editing. **Jonathan Martens:** Writing – review & editing. **Andrea M. Brunner:** Conceptualization, Writing – review & editing. **Jos Oomens:** Conceptualization, Writing - review & editing. **Giel Berden:** Conceptualization, Investigation, Writing – original draft.

Declaration of competing interest

The authors declare that they have no known competing financial interests or personal relationships that could have appeared to influence the work reported in this paper.

Data availability

Data will be made available on request.

Acknowledgements

We gratefully acknowledge the Nederlandse Organisatie voor Wetenschappelijk Onderzoek (NWO) for the support of the FELIX Laboratory through the research program “National Roadmap Grootschalige Wetenschappelijke Infrastructuur” 184.034.022 awarded to HFML-FELIX. We also thank the SURFsara Supercomputer Centre and the NWO ENW-domain for providing computational resources (NWO Rekentijd Grant 2021.055 awarded to J.O.).

Appendix A. Supplementary data

Supplementary data to this article can be found online at https://doi.org/10.1016/j.chemosphere.2023.140046.

References

Alotaibi, M.D., McKinley, A.J., Patterson, B.M., Reeder, A.Y., 2015. Benzotriazoles in the aquatic environment: a review of their occurrence, toxicity, degradation and analysis. Water, Air, Soil Pollut 226, 1–20.

Berden, G., Derksen, M., Houthuijs, K.J., Martens, J., Oomens, J., 2019. An automatic variable laser attenuator for IRMPD spectroscopy and analysis of power-dependence in fragmentation spectra. Int. J. Mass Spectrom. 443, 1–8.

Bernhardt, E.S., Rosi, E.J., Gessner, M.O., 2017. Synthetic chemicals as agents of global change. Front. Ecol. Environ. 15, 84–90.

Bottoni, P., Grenni, P., Lucentini, L., Caracciolo, A.B., 2013. Terbuthylazine and other triazines in Italian water resources. Microchem. J. 107, 136–142.

Brack, W., Barcelo Culleres, D., Boxall, A.B.A., Budzinski, H., Castiglioni, S., Covaci, A., Dulio, V., Escher, B.I., Fantke, P., Kandie, F., Fatta-Kassinos, D., Hernández, F.J., Hilscherová, K., Hollender, J., Hollert, H., Jahnke, A., Kasprzyk-Hordern, B., Khan, S.J., Kortenkamp, A., Kümmerer, K., Lalonde, B., Lamoree, M.H., Levi, Y., Lara Martín, P.A., Montagner, C.C., Mougin, C., Msagati, T., Oehlmann, J., Posthuma, L., Reid, M., Reinhard, M., Richardson, S.D., Rostkowski, P., Schymanski, E., Schneider, F., Slobodnik, J., Shibata, Y., Snyder, S.A., Fabriz Sodré, F., Teodorovic, I., Thomas, K.V., Umbuzeiro, G.A., Viet, P.H., Yew-Hoong, K.G., Zhang, X., Zuccato, E., 2022. One planet: one health. A call to support the initiative on a global science–policy body on chemicals and waste. Environ. Sci. Eur. 34, 21.

Brunner, A.M., Bertelkamp, C., Dingemans, M.M.L., Kolkman, A., Wols, B., Harmsen, D., Siegers, W., Martijn, B.J., Oorthuizen, W.A., Ter Laak, T.L., 2020. Integration of target analyses, non-target screening and effect-based monitoring to assess OMP related water quality changes in drinking water treatment. Sci. Total Environ. 705, 135779.

Buckingham, A.D., Del Bene, J.E., McDowell, S.A.C., 2008. The hydrogen bond. Chem. Phys. Lett. 463, 1–10.

Campos-Mañas, M.C., Plaza-Bolaños, P., Martínez-Piernas, A.B., Sánchez-Pérez, J.A., Agüera, A., 2019. Determination of pesticide levels in wastewater from an agro-food industry: target, suspect and transformation product analysis. Chemosphere 232, 152–163.

CASMI, 2022. https://fiehnlab.ucdavis.edu/casmi/casmi-2022-results accessed: 2023/03/09.

Crotti, S., Menicatti, M., Pallecchi, M., Bartolucci, G., 2021. Tandem Mass Spectrometry Approaches for Recognition of Isomeric Compounds Mixtures. Mass Spectrom. Rev., e21757

Del Bene, J.E., Jordan, M.J.T., 1999. Vibrational spectroscopy of the hydrogen bond: an ab initio quantum-chemical perspective. Int. Rev. Phys. Chem. 18, 119–162.

Dührkop, K., Fleischauer, M., Ludwig, M., Aksenov, A.A., Melnik, A.V., Meusel, M., Dorrestein, P.C., Rousu, J., Böcker, S., 2019. Sirius 4: a rapid tool for turning tandem mass spectra into metabolite structure information. Nat. Methods 16, 299–302.

Dührkop, K., Shen, H., Meusel, M., Rousu, J., Böcker, S., 2015. Searching molecular structure databases with tandem mass spectra using CSI: FingerID. Proc. Natl. Acad. Sci. U.S.A. 112, 12580–12585.

Ebejer, J.-P., Morris, G.M., Deane, C.M., 2012. Freely available conformer generation methods: how good are they? J. Chem. Inf. Model. 52, 1146–1158.

Engelke, U.F.H., Van Outersterp, R.E., Merx, J., Van Geenen, F.A.M.G., Van Rooij, A., Berden, G., Huigen, M.C.D.G., Kluijtmans, L.A.J., Peters, T.M.A., Al-Shekaili, H.H., 2021. Untargeted metabolomics and infrared ion spectroscopy identify biomarkers for pyridoxine-dependent epilepsy. J. Clin. Investig. 131.

Fang, Y., Karnjanapiboonwong, A., Chase, D.A., Wang, J., Morse, A.N., Anderson, T.A., 2012. Occurrence, fate, and persistence of gemfibrozil in water and soil. Environ. Toxicol. Chem. 31, 550–555.

Frisch, M.J., Trucks, G.W., Schlegel, H.B., Scuseria, G.E., Robb, M.A., Cheeseman, J.R., Scalmani, G., Barone, V., Petersson, G.A., Nakatsuji, H., Li, X., Caricato, M., Marenich, A.V., Bloino, J., Janesko, B.G., Gomperts, R., Mennucci, B., Hratchian, H. P., Ortiz, J.V., Izmaylov, A.F., Sonnenberg, J.L., Williams, Ding F., Lipparini, F., Egidi, F., Goings, J., Peng, B., Petrone, A., Henderson, T., Ranasinghe, D., Zakrzewski, V.G., Gao, J., Rega, N., Zheng, G., Liang, W., Hada, M., Ehara, M., Toyota, K., Fukuda, R., Hasegawa, J., Ishida, M., Nakajima, T., Honda, Y., Kitao, O., Nakai, H., Vreven, T., Throssell, K., Montgomery Jr., J.A., Peralta, J.E., Ogliaro, F., Bearpark, M.J., Heyd, J.J., Brothers, E.N., Kudin, K.N., Staroverov, V.N., Keith, T.A., Kobayashi, R., Normand, J., Raghavachari, K., Rendell, A.P., Burant, J.C., Iyengar, S. S., Tomasi, J., Cossi, M., Millam, J.M., Klene, M., Adamo, C., Cammi, R., Ochterski, J. W., Martin, R.L., Morokuma, K., Farkas, O., Foresman, J.B., Fox, D.J., 2016. Gaussian 16. Rev. C.01, Wallingford, CT.

Gámez, F., Avilés-Moreno, J.R., Berden, G., Oomens, J., Martínez-Haya, B., 2021. Proton in the ring: spectroscopy and dynamics of proton bonding in macrocycle cavities. Phys. Chem. Chem. Phys. 23, 21532–21543.

Halgren, T.A., 1996. Merck molecular force field. I. Basis, form, scope, parameterization, and performance of MMFF94. J. Comput. Chem. 17, 490–519.

Hollender, J., Schymanski, E.L., Singer, H.P., Ferguson, P.L., 2017. Nontarget screening with high resolution mass spectrometry in the environment: ready to go? Environ. Sci. Technol. 51, 11505–11512.

Houthuijs, D., Breugelmans, O.R.P., Baken, K.A., Sjerps, R.M.A., Schipper, M., van der Aa, M., van Wezel, A.P., 2022. Assessment of drinking water safety in The Netherlands using nationwide exposure and mortality data. Environ. Int. 166, 107356.

Houthuijs, K.J., Berden, G., Engelke, U.F.H., Gautam, V., Wishart, D.S., Wevers, R.A., Martens, J., Oomens, J., 2023. An in silico infrared spectral library of molecular ions for metabolite identification. Anal. Chem. 95, 8998–9005.

Hug, C., Ulrich, N., Schulze, T., Brack, W., Krauss, M., 2014. Identification of novel micropollutants in wastewater by a combination of suspect and nontarget screening. Environ. Pollut. 184, 25–32.

Kempkes, L.J.M., Martens, J., Grzetic, J., Berden, G., Oomens, J., 2016. Deamidation reactions of asparagine-and glutamine-containing dipeptides investigated by ion spectroscopy. J. Am. Soc. Mass Spectrom. 27, 1855–1869.

Kiefer, K., Du, L., Singer, H., Hollender, J., 2021. Identification of LC-HRMS nontarget signals in groundwater after source related prioritization. Water Res. 196, 116994.

Köppe, T., Jewell, K.S., Ehlig, B., Wick, A., Koschorreck, J., Ternes, T.A., 2023. Identification and trend analysis of organic cationic contaminants via non-target

screening in suspended particulate matter of the German rivers Rhine and Saar. Water Res. 229, 119304.
Kranenburg, R.F., van Geenen, F.A.M.G., Berden, G., Oomens, J., Martens, J., van Asten, A.C., 2020. Mass-spectrometry-based identification of synthetic drug isomers using infrared ion spectroscopy. Anal. Chem. 92, 7282–7288.
Landrum, G., 2006. RDKit: Open-Source Cheminformatics.
Little, J.L., Williams, A.J., Pshenichnov, A., Tkachenko, V., 2011. Identification of "known unknowns" utilizing accurate mass data and ChemSpider. J. Am. Soc. Mass Spectrom. 23, 179–185.
Martens, J., Berden, G., Gebhardt, C.R., Oomens, J., 2016. Infrared ion spectroscopy in a modified quadrupole ion trap mass spectrometer at the FELIX free electron laser laboratory. Rev. Sci. Instrum. 87, 103108.
Martens, J., Berden, G., van Outersterp, R.E., Kluijtmans, L.A.J., Engelke, U.F.H., van Karnebeek, C.D.M., Wevers, R.A., Oomens, J., 2017. Molecular identification in metabolomics using infrared ion spectroscopy. Sci. Rep. 7, 3363.
Martens, J., van Outersterp, R.E., Vreeken, R.J., Cuyckens, F., Coene, K.L.M., Engelke, U. F.H., Kluijtmans, L.A.J., Wevers, R.A., Buydens, L.M.C., Redlich, B., Berden, G., Oomens, J., 2020. Infrared ion spectroscopy: new opportunities for small-molecule identification in mass spectrometry-A tutorial perspective. Anal. Chim. Acta 1093, 1–15.
McEachran, A.D., Sobus, J.R., Williams, A.J., 2017. Identifying known unknowns using the US EPA's CompTox Chemistry Dashboard. Anal. Bioanal. Chem. 409, 1729–1735.
Morton, P.A., Fennell, C., Cassidy, R., Doody, D., Fenton, O., Mellander, P.E., Jordan, P., 2020. A Review of the Pesticide MCPA in the Land-water Environment and Emerging Research Needs, vol. 7. Wiley Interdiscip. Rev. Water, e1402.
Network, N., Aalizadeh, R., Alygizakis, N., Schymanski, E., Slobodnik, J., Fischer, S., Cirka, L., 2020. S0 | SUSDAT | Merged NORMAN Suspect List: SusDat. Zenodo, version NORMAN-SLE-S0. 0.2. 1.
Neveu, V., Moussy, A., Rouaix, H., Wedekind, R., Pon, A., Knox, C., Wishart, D.S., Scalbert, A., 2016. Exposome-Explorer: a Manually-Curated Database on Biomarkers of Exposure to Dietary and Environmental Factors. Nucleic Acids Res., p. gkw980
Oepts, D., Van der Meer, A.F.G., Van Amersfoort, P.W., 1995. The free-electron-laser user facility FELIX. Infrared Phys. Technol. 36, 297–308.
Panse, C., Sharma, S., Huguet, R., Vughs, D., Grossmann, J., Brunner, A.M., 2020. Ultraviolet photodissociation for non-target screening-based identification of organic micro-pollutants in water samples. Molecules 25, 4189.
Richardson, S.D., Thruston, A.D., Collette, T.W., Patterson, K.S., Lykins, B.W., Ireland, J. C., 1996. Identification of TiO2/UV disinfection byproducts in drinking water. Environ. Sci. Technol. 30, 3327–3334.
Ruff, M., Mueller, M.S., Loos, M., Singer, H.P., 2015. Quantitative target and systematic non-target analysis of polar organic micro-pollutants along the river Rhine using high-resolution mass-spectrometry–Identification of unknown sources and compounds. Water Res. 87, 145–154.
Ruttkies, C., Schymanski, E.L., Wolf, S., Hollender, J., Neumann, S., 2016. MetFrag relaunched: incorporating strategies beyond in silico fragmentation. J. Cheminf. 8, 1–16.
Schrimpe-Rutledge, A.C., Codreanu, S.G., Sherrod, S.D., McLean, J.A., 2016. Untargeted metabolomics strategies—challenges and emerging directions. J. Am. Soc. Mass Spectrom. 27, 1897–1905.
Schwarzenbach, R.P., Escher, B.I., Fenner, K., Hofstetter, T.B., Johnson, C.A., Von Gunten, U., Wehrli, B., 2006. The challenge of micropollutants in aquatic systems. Science 313, 1072–1077.
Schymanski, E.L., Jeon, J., Gulde, R., Fenner, K., Ruff, M., Singer, H.P., Hollender, J., 2014. Identifying small molecules via high resolution mass spectrometry: communicating confidence. Environ. Sci. Technol. 48, 2097–2098.
Steill, J.D., Oomens, J., 2009. Gas-phase deprotonation of p-hydroxybenzoic acid investigated by IR spectroscopy: solution-phase structure is retained upon ESI. J. Am. Chem. Soc. 131, 13570–13571.
Stephens, P.J., Devlin, F.J., Chabalowski, C.F., Frisch, M.J., 1994. Ab initio calculation of vibrational absorption and circular dichroism spectra using density functional force fields. J. Phys. Chem. 98, 11623–11627.
Thompson, T., Fawell, J., Kunikane, S., Jackson, D., Appleyard, S., Callan, P., Bartram, J., Kingston, P., 2007. Chemical Safety of Drinking Water: Assessing Priorities for Risk Management. World Health Organization.
Thruston, A.D., Richardson, S.D., McGuire, J.M., Collette, T.W., Trusty, C.D., 1991. Multispectral identiftcation of alkyl and chloroalkyl phosphates from an industrial effluent. J. Am. Soc. Mass Spectrom. 2, 419–426.
Tosco, P., Stiefl, N., Landrum, G., 2014. Bringing the MMFF force field to the RDKit: implementation and validation. J. Cheminf. 6, 37.
van Outersterp, R.E., Houthuijs, K.J., Berden, G., Engelke, U.F., Kluijtmans, L.A.J., Wevers, R.A., Coene, K.L.M., Oomens, J., Martens, J., 2019. Reference-standard free metabolite identification using infrared ion spectroscopy. Int. J. Mass Spectrom. 443, 77–85.
van Outersterp, R.E., Martens, J., Berden, G., Lubin, A., Cuyckens, F., Oomens, J., 2022. Identification of drug metabolites with infrared ion spectroscopy–application to midazolam in vitro metabolism. Chem. Methods, e202200068.
van Outersterp, R.E., Oosterhout, J., Gebhardt, C.R., Berden, G., Engelke, U.F.H., Wevers, R.A., Cuyckens, F., Oomens, J., Martens, J., 2023. Targeted small-molecule identification using heartcutting liquid chromatography–infrared ion spectroscopy. Anal. Chem. 95, 3406–3413.
Verliefde, A., Cornelissen, E., Amy, G., Van der Bruggen, B., Van Dijk, H., 2007. Priority organic micropollutants in water sources in Flanders and The Netherlands and assessment of removal possibilities with nanofiltration. Environ. Pollut. 146, 281–289.
Villanueva, C.M., Kogevinas, M., Cordier, S., Templeton, M.R., Vermeulen, R., Nuckols, J.R., Nieuwenhuijsen, M.J., Levallois, P., 2014. Assessing exposure and health consequences of chemicals in drinking water: current state of knowledge and research needs. Environ. Health Perspect. 122, 213–221.
Vink, M.J.A., van Geenen, F.A.M.G., Berden, G., O'Riordan, T.J.C., Howe, P.W., Oomens, J., Perry, S.J., Martens, J., 2022. Structural elucidation of agrochemicals and related derivatives using infrared ion spectroscopy. Environ. Sci. Technol. 56, 15563–15572.
Walhout, E.Q., Dorn, S.E., Martens, J., Berden, G., Oomens, J., Cheong, P.H.-Y., Kroll, J. H., O'Brien, R.E., 2019. Infrared ion spectroscopy of environmental organic mixtures: probing the composition of α-pinene secondary organic aerosol. Environ. Sci. Technol. 53, 7604–7612.
Wang, F., Liigand, J., Tian, S., Arndt, D., Greiner, R., Wishart, D.S., 2021. CFM-ID 4.0: more accurate ESI-MS/MS spectral prediction and compound identification. Anal. Chem. 93, 11692–11700.
Wang, S., Miltner, A., Kästner, M., Schäffer, A., Nowak, K.M., 2017. Transformation of metamitron in water-sediment systems: detailed insight into the biodegradation processes. Sci. Total Environ. 578, 100–108.
Warnke, S., Seo, J., Boschmans, J., Sobott, F., Scrivens, J.H., Bleiholder, C., Bowers, M.T., Gewinner, S., Schollkopf, W., Pagel, K., Von Helden, G., 2015. Protomers of benzocaine: solvent and permittivity dependence. J. Am. Chem. Soc. 137, 4236–4242.
Weininger, D., 1988. SMILES, a chemical language and information system. 1. Introduction to methodology and encoding rules. J. Chem. Inf. Comput. Sci. 28, 31–36.
Wishart, D.S., Feunang, Y.D., Marcu, A., Guo, A.C., Liang, K., Vázquez-Fresno, R., Sajed, T., Johnson, D., Li, C., Karu, N., 2018. Hmdb 4.0: the human metabolome database for 2018. Nucleic Acids Res. 46, D608–D617.
Zheng, K.-X., Liu, C.-H., Wang, S., Tzou, Y.-M., Chiang, C.-M., Lin, S.-R., Yang, H.-Y., Wu, J.J., Chuang, Y.-H., 2023. Evaluating the release and metabolism of ricinine from castor cake fertilizer in soils using a LC-QTOF/MS coupled with SIRIUS workflow. Chemosphere 310, 136865.
Zimmerman, L.R., Schneider, R.J., Thurman, E.M., 2002. Analysis and detection of the herbicides dimethenamid and flufenacet and their sulfonic and oxanilic acid degradates in natural water. J. Agric. Food Chem. 50, 1045–1052.